7. Changes in mountain water resources

7.1 Experimental Hydrological Database for Apennine Basins: a support to enhance the knowledge on hydrological cycle

S. Barbetta[1], M. Borga[2], L. Brocca[1], S. Camici[1], L. Ciabatta[1], C. Corradini[1], L. Marchi[1], T. Moramarco[1]

[1]*National Research Council, Research Institute for Geo-hydrological Protection, Italy*
[2]*University of Padova, Department of Land Environment, Agriculture and Forestry, Italy*

7.1.1 Introduction

New monitoring techniques (in situ and remote sensing) for key hydrologic variables, such as rainfall and temperature, on the one hand, and soil moisture and river discharge, on the other hand, are critically important in mountain areas to investigate the hydrological cycle. Moreover, the advanced technologies (radar, remote sensing), which are attractive for the derivation of spatially distributed hydrological information, require data validation with in situ measurements. On this basis, a reliable hydro-meteorological network is essentials for the advance in the knowledge of runoff generation process, which is fundamental for both water resources management and hydraulic risk prevention and mitigation.

7.1.2 Objective

In this context, the set-up of a hydro-meteorological database as a component of the 'Network of Excellence' to monitor mountain areas and to improve the knowledge of the hydrological cycle is crucial. This work proposes the "Database Idrologico Bacini Appenninici" (DIBA), developed within NextData-CNR program, funded by the Italian Ministry of Education, University and Research (MIUR). DIBA is intended to provide a useful hydro-meteorological dataset to leverage for analyses concerning the climate and the main hydrological processes in catchments using ground and satellite observations. DIBA has been implemented by using the MVC architecture based on the ZEND v1 PHP framework and is structured as a WEB-GIS platform allowing, on the one hand, a wide sharing and participation of data via WEB and, on the other hand, a better use of data itself by GIS. The latter, is mainly applied to the identification of temporal-space pattern of hydrological variables and the inventory of thematic maps.

7.1.3 Data Structure

DIBA was built on the basis of the collection of hydro-meteorological time series of two pilot Apennines basins: the Upper-Chiascio basin (460 km^2), in central Italy, and the Magra basin (1717 km^2), in central-northern Italy. Time series recorded by 66 rain-gauges, 63 thermometers, 8 hydrometric stations, 3 meteorological stations and one soil moisture station are included in the WEB-GIS platform. For the Chiascio basin, the recorded half-hourly data are relative to different availability periods of the monitoring stations (time series last from 7 to 26 years) and daily data are also available. For the Magra basin, different hourly and daily time series are available at the stations, which are currently managed by two Regions (Liguria and Tuscany).

For the two pilot basins, DIBA also holds rainfall data from radar and satellite (TMPA rainfall product, H05 rainfall product) as well as soil moisture satellite products (ASCAT, AMSR-E, MODIS, SMOS). In addition, the database allows to manage thematic maps (channel network, sub-basins, land use, lithology, SCS Curve Number).
Climate scenarios are also available in the platform for Global Circulation Models such as HadCM3, CMCC-CM and EC-Earth for the reference period (1960-1990) and for downscaled future scenarios. Experimental campaigns for soil moisture monitoring in hillslope portions by Time Domain Reflectometry and streamflow measurements in selected river sites using non-contact radar sensors were carried out during the 2014-2015 project period to feed DIBA and to be used for hydrological analysis, as shown in the following section. The structure of DIBA is shown in Figure 1.

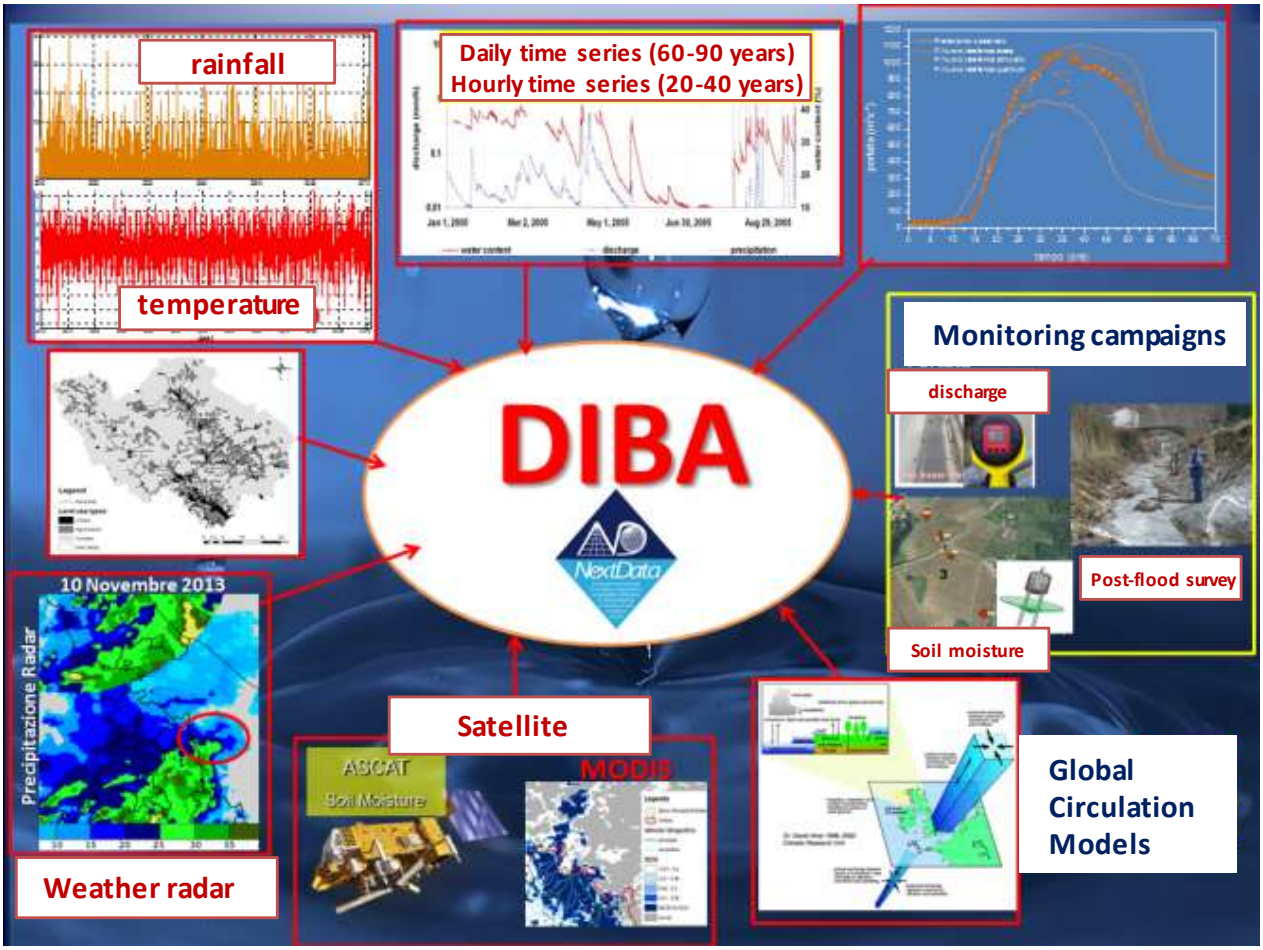

Figure 1. *DIBA structure.*

All features (basin boundaries, hydro-meteorological stations, hydrography, land use, etc.) are geo-referenced on Google Map providing tables with their locations in terms of latitude and longitude.
Data have been verified through data quality control procedures and the reconstruction of malfunction periods to obtain a reliable assessment of hydrological variables. The precipitation and temperature control procedure was articulated into five different steps that, by evaluating the consistency of the data with the station's statistical properties (mean, variance, maximum observed) and neighboring stations, assigns a quality code of data. For hydrometric data, the quality control mainly concerned the identification of non-operational periods that were corrected on the basis of

linear approaches for short periods or on observations of upstream/downstream hydrometric stations. The control also concerned the offset of the stations which, for some of them, have had variations during the recording period.

7.1.4 Data analysis

The data made available in the WEB-GIS platform of DIBA, can be used for interesting scientific investigations.

An important outcome of the data analysis derives from the field measurements carried out in 2014-2015 for monitoring the saturation degree in the Chiascio River basin. Figure 2 shows the degree of saturation in the selected hillslope portions during the mentioned campaigns; as it can be seen, the areas more/less wet remained always the same ones, highlighting how the spatial variability of degree of saturation is strictly related with that of soil structure and topography. Moreover, a high correlation (R>0.8) is found between the average soil moisture of hillslope and surface velocity of river flow at outlet of basin.

The hydro-meteorological data have been also used to analyze the main hydrological processes in the two pilot areas. Specifically, DIBA contains data referring to the application of a continuous semi-distributed hydrological model, named MISDc ('Modello Idrologico Semi-Distribuito in continuo'), and developed by CNR-IRPI (Brocca et al., 2011). MISDc uses a two-layers scheme of the soil and is initialized by rainfall and temperature data. The temporal evolution of the two independent soil water states of the basin and the discharge at the basin outlet have been simulated and embedded in DIBA. MISDc provided the initial soil moisture state before of floods which is of paramount importance to identify the degree of saturation to be used for analysis.

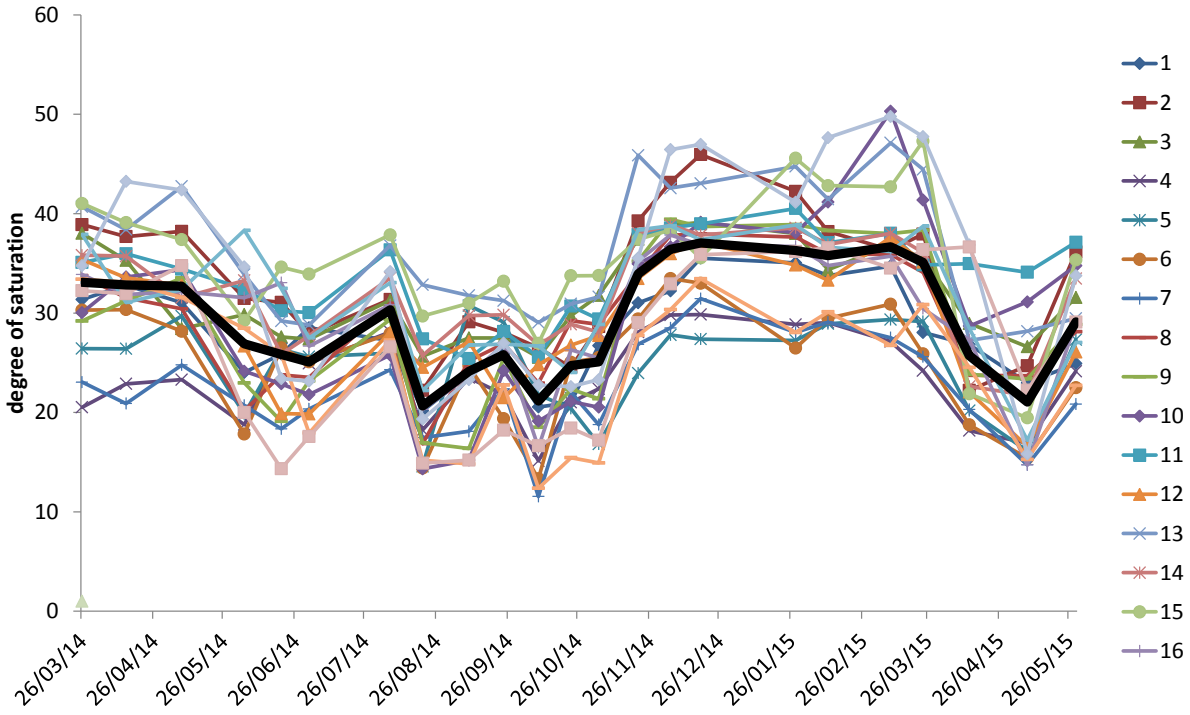

***Figure 2**. Chiascio River basin: degree of saturation of selected hillslope portions during 16 campaigns. The black line represents the mean of the 16 measurements.*

The hydrological model was applied to the two monitored sections in the Chiascio River basin (Branca and La Chiusa, subtended drainage area equal to 166 and 406 km^2, respectively) and to the Magra River at the Calamazza stream-gauge, which drains most of basin area and is critical for flooding. The obtained results show the good performance of the hydrological model in simulating the observed discharge (see Table 1). For example, the Nash-Sutcliffe efficiency, NSE, (Nash and Sutcliffe, 1970) was satisfactory for the calibration analysis for Branca and Calamazza section with a value equal to 0.924 and 0.804, respectively. Also the computed values of *NSE* adapted for high-flow conditions, *ANSE,* and the coefficient of determination, R^2, clearly indicate a good accuracy of the model (*ANSE*=0.961 and 0.861, R^2=0.926 and 0.911 for Branca and Calamazza sections, respectively). When La Chiusa section is of concern, a lower accuracy is observed (*NSE*=0.66, *ANSE*= 0.682, R^2=0.775), but it is worth mentioning that the rating curve for La Chiusa section could be affected by uncertainties for medium-high stage values.

By way of example, Figures 3-4 show the results of the hydrological simulation for the watershed subtended by Branca and Calamazza gauged section, respectively. Specifically, for the basin subtended by Branca, the values of all the selected metrics are very high in calibration (see Figure 3). When the largest watershed subtended by La Chiusa site is considered, the short period of available data was entirely used for calibrating the hydrological model parameters. In this case, we find a lower performance of MISDc that, however, was able to simulate the trend of the recorded data.

The good performance of the model is also demonstrated by the comparison shown in the lower panel of Figure 4 for the watershed subtended by Calamazza section.

The calibrated MISDc model was also applied to identify climate scenarios by using as input data the selected GCM models, downscaled with observed hydrological time series. The analysis also identified hydrological trends and the ensuing runoff regime scenarios expected in the next decades.

Finally, the project identified appropriate guidelines for river flood response assessment through post-flash flood surveys (Gaume and Borga, 2008). The method used in Intensive Post-Event Campaigns (IPEC) (Marchi et al., 2009) provided data on flood response (peak discharge, time evolution of the flood, interactions with slope instability and geomorphic processes in channels), thus complementing the harmonization of hydro-meteorological database and the collection of soil moisture and flow velocity data in the two basins. An approach based on the linear error analysis of the Manning-Strickler equation, applied for post-flood estimate of peak discharge in the IPECs, was developed to assess the observational errors associated to topographic measurements, roughness coefficient estimation and to geomorphic changes caused by the flood in the surveyed sections (Amponsah et al., 2016).

Basin	Period	NSE	ANSE	R^2	KGE
Branca (Chiascio River)	Calibration (May 2008-Dec2014)	0.827	0.907	0.835	0.914
	Calibration (May 2008-Dec 2010)	0.924	0.961	0.926	0.962
	Validation (Jan 2011-Dec 2014)	0.735	0.829	0.773	0.603

La Chiusa (Chiascio River)	Calibration (Oct 2011-Nov 2013)	0.659	0.682	0.775	0.791
Calamazza (Magra River)	Calibration (May 2008-Dec2014)	0.827	0.907	0.835	0.914
	Calibration (May 2008-Dec 2010)	0.924	0.961	0.926	0.962
	Validation (Jan 2011-Dec 2014)	0.735	0.829	0.773	0.603

***Table 1**. Performance indexes obtained for the hydrological model application for the pilot areas (Nash-Sutcliffe efficiency, NSE; NSE adapted for high-flow conditions, ANSE; Coefficient of determination, R^2; Kling-Gupta efficiency, KGE).*

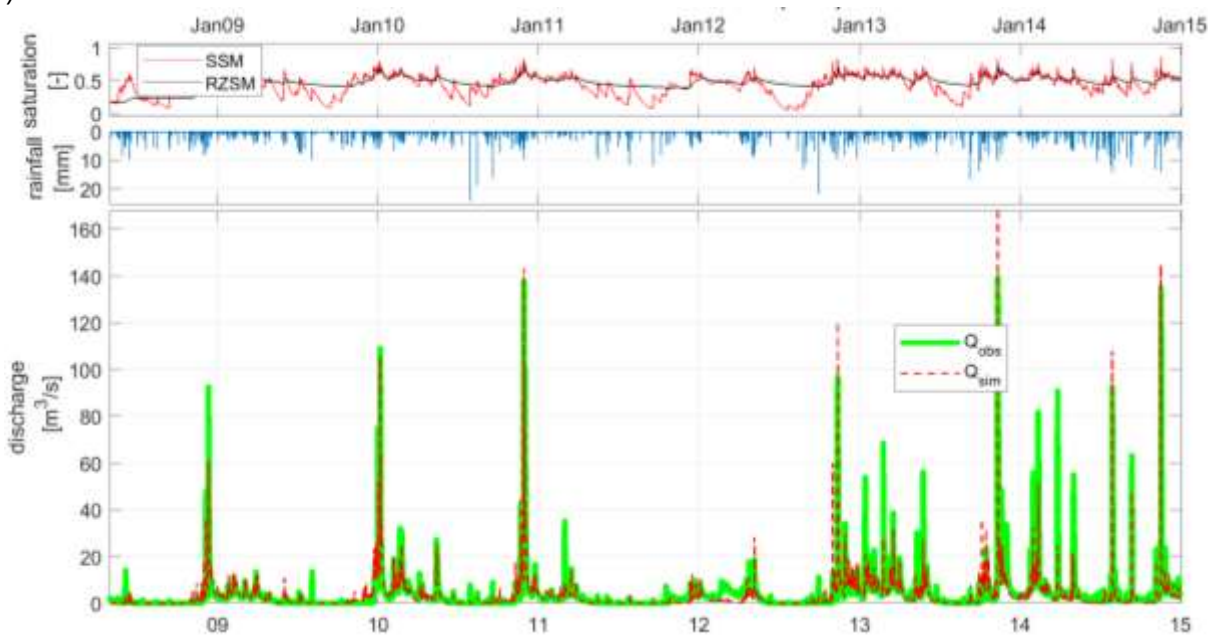

***Figure 3.** Branca section, calibration period May 2008-December 2014: upper panel) soil saturation degree for the surface layer (SSM) and for the root zone layer (RZSM); middle panel) mean areal observed rainfall; lower panel) comparison between observed and simulated discharge.*

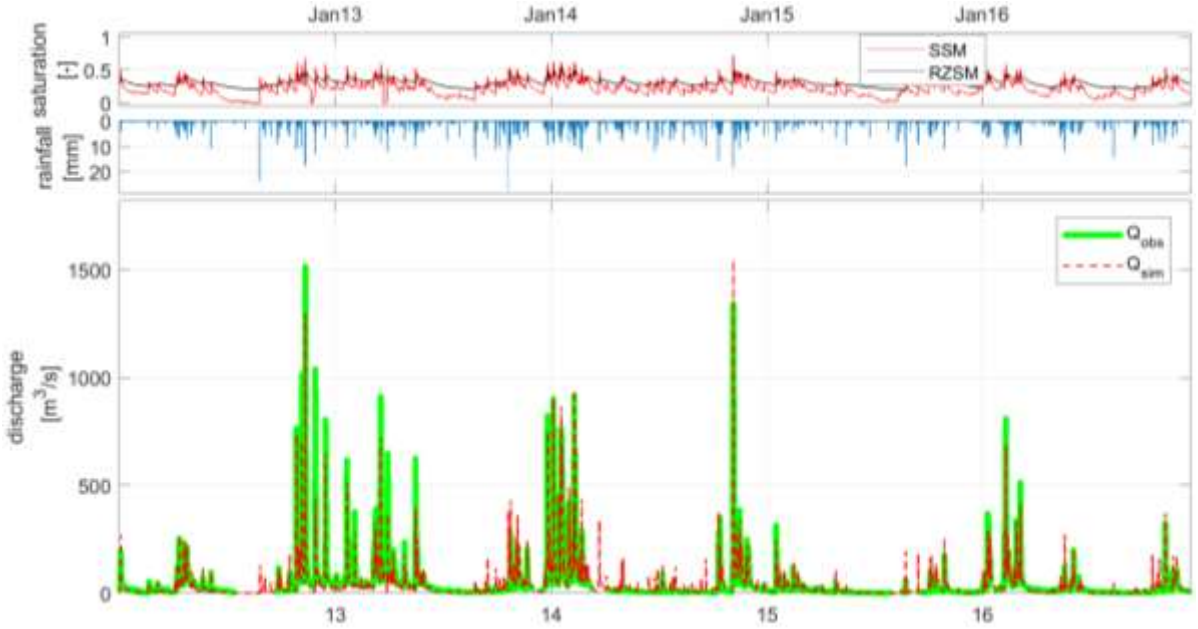

***Figure 4.** Calamazza section, calibration period January 2012-December 2016: upper panel) soil saturation degree for the surface layer (SSM) and for the root zone layer (RZSM); middle panel) mean areal observed rainfall; lower panel) comparison between observed and simulated discharge.*

7.1.5 Conclusions

Activities planned in DIBA project were efficiently developed and meaningful results were achieved in terms of collection, organization and analysis of the available hydro-meteorological and climate data. The database, made available through a WEB-GIS platform, was included as a component of the "Network of Excellence" for the monitoring of mountain areas in the context of the NextData programme. DIBA can be conveniently adopted for analyses of hydrological processes identifying the hydrological cycle as well as for the characterization of the meteo-climate evolution in different mountain areas.

7.2 Relationships between atmospheric circulation and river flow

S. Gualdi[1], M. Zampieri[1, 2]

[1]*Euro Mediterranean Center on Climate Change (CMCC), Bologna, Italy*

[2]*Joint Research Center (JRC) Ispra, Italy*

The Alps represent the most important freshwater supply of continental Europe, since the Rhine, Po, Rhone and several tributaries of the Danube originate here. Due to their high elevation, the hydrological cycle of the Alps is largely influenced by snow. Snow precipitation on the Alpine region, thus, has important repercussions both on environment and society (Beniston 2012; Barnett et al., 2005).

Air temperature variations can alter the partition of solid to liquid precipitation (Scherrer et al., 2004; Serquet et al., 2011) and the spring snowmelt timing, determining the length of the snowy season (Laternser and Schneebeli, 2003).

Global warming is believed to be responsible for the reduction of snow amount and duration over the Alps, as a rapid shortening of the snowy season has been observed in the past few decades (Serquet et al., 2011). This trend is projected to continue during the 21st century in the climate change scenarios with increasing greenhouse gas concentrations (Beniston, 2012).

The long–term trend of reduction of spring snowfall, which determines the length of the snowy season, can be explained in large part by the warming of the Alps (Scherrer et al., 2013). However, superimposed on this long–term trend there is a low–frequency variability of snowfall associated with, natural, multi–decadal changes in the large–scale circulation (Trenberth et al., 2007). The amplitude of this natural low–frequency variation might be relatively large, determining rapid and substantial changes of snowfall. Therefore, decadal variations in teleconnections can considerably complicate the interpretation of the climate change signal, and the snowfall trend computed over a few decades can be larger than the effects that might be attributed solely to climate change.

This was already evidenced in connection with the retreat of glaciers in the Tropics (Francou et al., 2003; Kaser et al., 2004).

Slow natural fluctuations of the atmospheric circulation, affecting winter snowfall over the Alpine region, have already been documented. For example, the recent tendency toward a predominantly positive phase of the North Atlantic Oscillation (NAO; Hurrell, 1995) corresponded to high-pressure, warm and dry weather conditions, unfavourable to snow over the Alps, which has decreased since the 1980s at elevations below 1500–2000 m (see e.g. Beniston, 1997; Bartolini et al., 2001; Laternser

and Schneebeli, 2003; Scherrer and Appenzeller, 2006; Marty, 2008; Durand et al., 2009; Valt and Cianfarra, 2010).

In the framework of NextData, Zampieri et al. (2013) have shown that the Atlantic Multi-decadal Oscillation (AMO; Schlesinger and Ramankutty, 1994), which has been recently identified as one of the main natural drivers of the low–frequency variability of the European climate (Sutton and Dong, 2012; Huss et al., 2010), can induce substantial low–frequency variations of spring snowfall over the Alps.

In particular, using the HISTALP snowfall reconstruction over the past two centuries (Auer et al., 2007; Brunetti et al., 2009), direct observations in the Swiss and French Alps and the 20th Century Reanalysis provided by the NOAA/OAR/ESRL PSD (Compo et al., 2011; www.esrl.noaa.gov/psd/), Zampieri et al. (2013) have found a transition from abundant to reduced spring snowfall regimes in the middle 1990s, corresponding to the last transition toward a warm phase of the AMO. According to their findings, there have been two similar pairs of synchronous shifts in the past 150 years, where snowfall regime variations, determined by changes in both total precipitation and near surface temperature, appear to occur concomitantly with changes of the AMO phase.

Specifically, they found that transitions from cold to warm phases of the AMO could produce significant snowfall reductions in wider areas at relatively low elevations of the Alpine region. The signal of snowfall change appears to be more robust in the western Alps, where the AMO transition is accompanied by a spring snowfall reduction as large as 20–30% of the total spring snowfall. According to the 20th Century Reanalysis, precipitation anomalies can be explained by changes of circulation connected to the AMO transitions.

In the case of cold to warm AMO transitions, it consists of a high-pressure ridge pattern between two anomalous lows over the northeast Atlantic Ocean and north-eastern Europe, in agreement with Sutton and Dong (2012). Temperature anomalies over Western Europe due to advection of Northern Atlantic air are emphasized by the cloudiness anomalies.

The changes in snowfall over the Alps, both long–term trends and low–frequency variations, have obvious effects on the characteristics of the discharge of the main Alpine rivers, such as Danube, Rhine, Rhone and Po. In a study conducted within NextData, Zampieri et al. (2015) have investigated how changes in the seasonality of total precipitation can significantly affect the hydrological cycle of the Alpine region. To this aim, river discharge monthly time-series have been obtained by combining data from different sources, mainly from the Global Runoff Data Center (GRDC, http://www.bafg.de) and from local regional authorities. Besides, gridded datasets of monthly, homogenised surface observations from the HISTALP project have been used at 10′ resolution from 1801 to 2003 for precipitation, and from 1780 to 2008 for temperature (Efthymiadis et al., 2006; Auer et al., 2007; Brunetti et al., 2009) in the Alpine region (4–19E, 43–49N). To strengthen their results on the precipitation timings, Zampieri et al. (2015) integrated the analysis of total precipitation using the global gridded observations from the Climate Research Unit (CRU) TS 3.10.01 dataset for the period 1901–2009. This was available at a resolution of 0.5 by 0.5° (Mitchell and Jones, 2005). Furthermore, as an independent dataset, Zampieri et al. (2015) adopted the corresponding product from the 20th Century Reanalysis Version 2, available from 1871 to present, at 2° spatial resolution (Compo et al., 2011). The results obtained with these datasets were compared to those of HISTALP during the overlapping period.

Their results, consistent with previous findings (Pfister et al., 2006; Birsan et al., 2005; Stahl et al., 2010), show a tendency of increasing winter runoff with respect to other seasons. However, compared to other studies, Zampieri et al. (2015) have undertaken a more extended and in depth investigation that allowed disentangling the contribution of the long–term trend and the decadal variability. In particular, they showed that the long–term trend of earlier spring river discharge timings is mostly explained by the change of seasonality of precipitation and the increase of its liquid portion, while snowmelt is better suited to explain the low-frequency (decadal) fluctuations. This peculiarity of the Alpine climate change, highlighted in Zampieri et al. (2015), differs from the common perception that earlier spring discharges are mainly due to earlier snowmelt and larger rainfall in relation to total precipitation ratio caused by global warming (see e.g. Barnett et al., 2005; Moore et al., 2007; Pederson et al., 2011).

Zampieri et al. (2015) results show a consistent earlier spring discharge of more than two weeks per century in the basins located north of the Alps (Rhine and Danube), and more than three weeks per century in the basins located to the south (Rhone and Po). In the Po basin, a significant role in this earlier trend is also played by the long-term tendency of an increased spring liquid precipitation ratio, in line with the general warming trend observed over the Alpine region (Serquet et al., 2011; Beniston, 2012). The low-frequency (decadal) fluctuations of spring discharge timings can be partly explained by changes in the snowmelt timings, especially in the Rhine and Po basins, and partly by changes in the liquid precipitation ratio in all basins except the Rhone and the Po. In particular, Zampieri et al. (2015) have observed a shift towards a pluvial-torrential regime with respect to the snowmelt dominated regime that has characterized the southern basins since the 1970s and the northern basins since the 1980s. These changes can amplify the risk of flooding (e.g., Dobler et al., 2012). A limitation of Zampieri et al. (2015) analysis is the neglect of soil moisture and groundwater processes (Tague and Grant, 2009; Mayer and Naman, 2011) and glacier ice melting (Kaser et al., 2010), because of the lack of observed data at the scales considered in their study. However, as the cited papers state, these aspects have only minor effects on the processes leading to the peak discharge maximum. Besides, the intensive water management in the Alpine region might also play a role in modulating river discharge. However, though this effect is difficult to quantify, Zampieri et al. (2015) show that built hydraulic structures do not appear to affect significantly the trend and the low–frequency variability of the spring peak timings, in all basins considered. Moreover, it is unlikely that human modification of land and hydrology could produce the common features that they found in the different basins, which are regulated by different authorities and subject to different land–use and water management practices. Therefore, most of the observed changes in Alpine river discharge can be attributed to climate change.

Future trends and changes in the hydrological cycle may also affect, and be influenced in turn by, the occurrence of heat waves. Runoff production and river discharge, in fact, is expected to be anti-correlated with anomalous hot weather because of a variety of reasons and feedbacks processes. In fact, heat waves cause an increase of evapotranspiration that reduces soil moisture, and soil moisture deficit itself can act as an amplifier of heat waves amplitude (e.g. Seneviratne et al., 2010). Moreover, in several regions as Europe and the Mediterranean, soil dryness can represent a precursor of heat waves in the summer season (Vautard et al., 2007; Zampieri et al., 2009), while

circulation anomalies producing meteorological and soil dryness can be simply the same connected to hot weather (Lionello, 2012).

Whether heat waves have increased in frequency, duration, and/or amplitude is a much debated issue in climate change science. Given the limited data availability on a daily time scale, most studies of heat waves are based on data since 1950. On a global scale, there is a medium level of confidence that they have increased in frequency and/or duration (IPCC, 2013), and is likely that the frequency of heat waves has increased in large parts of Europe (e.g., Perkins et al., 2012). Concerning the future, if the atmospheric greenhouse gases concentration will continue to increase, it is very likely that heat waves will occur with a higher frequency, intensity and duration in the coming decades (IPCC, 2013; Russo et al., 2014).

In another NextData study, Zampieri et al. (2016) have explored the effects of heat waves on the Alpine river discharge. To this aim, they used 20th Century Reanalyses from the National Oceanic and Atmospheric Administration (NOAA 20CR–2, 20CR–2C; Compo et al. 2011, 2015) and from the European Centre for Medium-Range Weather Forecasts (ECMWF ERA–20C, Poli et al., 2016) to explore the link between low–frequency variation of heat waves and river discharge in the Alps. Specifically, they provide a cross–comparison of the Heat Wave Magnitude Index daily (HWMId, Russo et al., 2015) time series (computed from the reanalyses of the 20th Century Reanalyses 20CR–2, 20CR–2C and ERA–20C), with the river discharge originated over the Alps (computed using the GRDC data; see also Zampieri et al., 2015).

The HWMId is defined as the maximum magnitude of the heat waves in a year, where a heat wave is a period of at least 3 consecutive days with maximum temperature exceeding the daily threshold for the reference period (1981–2010). The threshold is defined as the 90th percentile of the daily maximum temperature, centred on a 31–day window. The HWMId is the sum of the magnitude of the consecutive days composing a heat wave, with daily magnitude calculated by means of the magnitude daily function (Md) as defined in Russo et al. (2015).

Figure 5 shows the time-series of the HMWId computed over the Alps for the three reanalysis, their weighted mean, and the total discharge contributing to the Rhine, Danube, Rhone and Po river. From these results, it appears evident that variations in heat waves occurrence and magnitude are significantly correlated to negative anomalies of river discharge originated over the Alps.

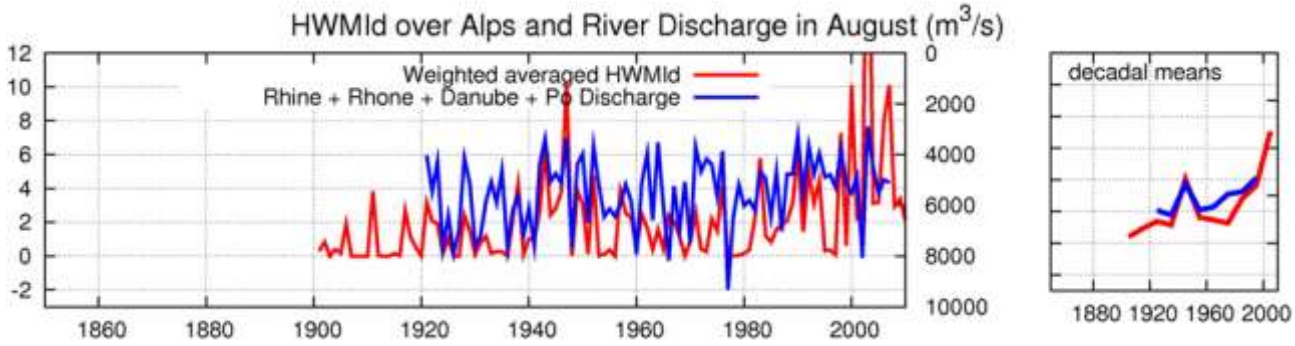

***Figure 5**. Time series of HWMId computed over the area from 5E to 15E and from 44N to 49N, covering approximately the basins of the Rhine, Rhone, Danube and Po rivers relative to the gauge station located at Basel, Beaucaire, Bratislava and Pontelagoscuro, respectively (in red, left axes), and the sum of the river discharge (in blue, right axes, in cubic meters per second, see Zampieri et al. (2015) for a description of the river basins, stations and data). Left panel shows the weighted mean of annual values of HWMId as obtained from the 20th Century Reanalysis version 2 (20CR-2), the 20th Century Reanalysis version 2c (20CR-2c) and the ECMWF reanalysis (ERA-20C). Right panel shows the decadal mean time–series of the left panel plots (same axes as in the left panel).*

The multiple reasons discussed above, are indeed responsible for a high level of consistency between heat waves occurrence and negative river discharge anomaly, as expected. From the annual values, it is possible to infer a significant (anti)correlation of the data.

The correlation values are shown in Table 2. Linear correlations are −0.72 for the weighted mean index, −0.62 for 20CR-2, −0.56 for 20CR-2c and −0.64 for ERA-20C if computed until 1960, when the majority of the dams and hydraulic structures where built (Zampieri et al., 2015).

Lower correlations, around −0.5, characterize the full time-series (see the second row of Table 2). Visual inspection of the decadal means (Figure 5, right panel) also reveals a high level of consistency, especially regarding the warm-dry event in the 1950s and the trend characterizing the following decades.

Period	Weighted mean	20CR-2	20CR-2c	ERA-20C
1921–1960	−0.72	−0.62	−0.56	−0.64
1921–2007	−0.48	−0.54	−0.46	−0.39

Table 2. *Linear correlations between the HWMI and river discharge computed over the Alps (5E–15E, 44N–49N) and shown in Fig. 5. The first row shows the results of the correlations computed until 1960, when most of the hydraulic structures were built (Zampieri et al., 2015). The second row shows the results computed over the entire time-series.*

7.3 Dynamics of groundwater systems

M. Doveri[1], A. Irace[1], M. Lelli[1], G. Masetti[1], M. Menichini[1], B. Nisi[1], B. Raco[1]

[1]*Institute of Geosciences and Earth Resources, National Research Council, Italy*

7.3.1 Introduction

Groundwater represents the main resource in term of water supply and in many areas it is the most important and safest source for drinking water, as in the European countries, where groundwater exploitation provides water for human consumption for 70% of the population on average (Doveri et al., 2016 and references therein). Despite this, and unlike surface waters, groundwater bodies have not been widely studied, and there is a general paucity of information, especially in relation to climate change. Although groundwater are more resilient to climate change than surface water, they are however affected both directly and indirectly (Tylor et al., 2013), and an increasing of knowledge including the estimation of the entity of the climate effects is mandatory for a reliable management of this crucial resource.

Within the WP1.2 of the NextData project, we dealt with groundwater quantity and quality issues, referring to three selected aquifer systems that develop (Figure 6) in Apennines (Mt. Amiata and Apuan Alps systems) and Alpine zones (foothill system of the Piedmont). The selection of these systems, based on the different types of hydrodynamic conditions that they offer, thus providing a wide casuistry of groundwater behaviour and typology of survey approach and data analysis to be adopted. Indeed, one of the aim was to provide working approaches as reference strategies for investigating mountain aquifers.

7.3.2 Methodology

The activities were carried out through three main steps: *i)* definition of the aquifers conceptual model; *ii)* analysis of monitoring data for verifying trends in groundwater quantity and quality; *iii)* development of numerical models for reproducing present and past behaviour of groundwater flow, as well as for providing a tool to be used for groundwater forecasting as a function of the climate scenarios.

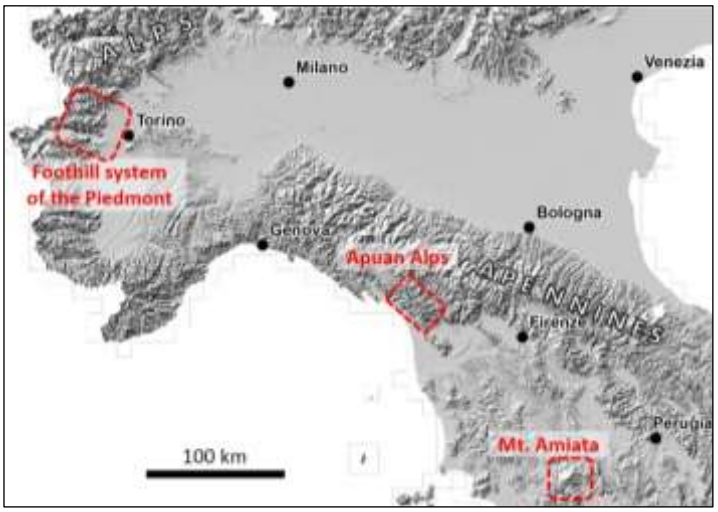

Figure 6. *Apennines and Alps zones in which aquifer systems exanimated in the project extend.*

The first step is essential for steering the next two steps towards consistent results. The conceptual models have been defined by considering geological, hydrogeological and hydraulic-hydrodynamic features, as well as chemistry and water isotopes signature in groundwater. Data and information derive from studies and researches chiefly performed in close cooperation with water management companies and authorities, as well as from monitoring activities institutionally

performed by regional governments and environmental agencies. This comprehensive approach, enable to include in the models the kind and the geometry of rocks hosting groundwater and their hydraulic properties, the feeding areas and the arrangement of groundwater flow, the representativeness of water points (wells and springs) respect to the main groundwater bodies, the seasonal evolution of groundwater quantity, the chemical features and the processes that originate them.

Considering the information from conceptual models, springs and wells were selected for performing a trend analysis of water quantity and quality, as well as an evaluation of local chemical background values. For the latter, probability diagrams (Sinclair, 1986 and references therein) were elaborated to recognize the presence of several populations in a given dataset and to divide it into individual populations to be associated with a process that has generated the specific range of chemical concentrations. For each population, the threshold value was placed at the 95th percentile, which is considered representative of natural processes and not influenced by anthropogenic effects. The trend analysis was performed on parameters considered significant for the system under study, and particularly it has concerned both chemical compounds concentration and water quantity (i.e. springs flow rate, water level in piezometers). The following statistical method was adopted: *i)* analysis of the frequency distribution of the considered parameters, by means of the Shapiro-Wilk and Lilliefors tests (Razali & Wah, 2011); *ii)* analysis of the presence of potential outlier values, evaluated by Rosner and Dixon tests (Rosner, 1975; Rosner 1983; Rousseeuw and Leroy, 1987; Singh and Nocerino, 1995); *iii)* analysis of the presence of temporal trends through the non-parametric tests of Theis-Sen (Wilcox and Rand, 2001; Sen, 1968) compared with Ordinary Last Square (OLS) regression.

As a consequence of the availability of data and information and aquifers hydrodynamic conditions, two main types of numerical models were developed for reproducing the quantitative behaviour of groundwater with respect to hydroclimate parameters: *i)* empirical models; and *ii)* physically based models. The type of model was consequence of the hydrodynamic conditions of aquifers and the availability of data and information. With the empirical models, the relations that link the aquifer yield (e.g. spring flowrate) with the hydroclimate variables was described by functions (f) of the type $Q = f(R, T, ER)$, where *Q* is the flowrate, *R* is the rainfall, *T* is temperature and *ER* is the effective rainfall (considering evapotranspiration). Firstly, a statistical study of data time series was performed by means of a critical analysis of possible outliers, the research of variables autocorrelations, the Fourier analysis to find cyclic events, and the cross-correlation techniques among variables. Afterwards, several regression models were implemented considering different options of time lag and relation between flow rates and hydroclimate parameters. The robustness of the models was then verified by the analysis of residuals. For the physically-based approach, a 3D model was realized using the Modflow code (Harbaugh et al., 2000), thus discretizing the aquifer systems by cells and inserting hydraulic properties, boundary and initial conditions (e.g. water head at boundaries of the model area, rivers, etc.) and considering the external stresses (e.g. recharge, pumping rates, etc.). The calibration of the model was performed respect to the observed water head at target wells or piezometers.

7.3.3 Results and discussion

Main features of the aquifer systems under study

Three aquifer systems were taken into account. The volcanic aquifer of the Mt. Amiata, in Central Apennines, the carbonate aquifer of the Apuan Alps, in North Apennines, and the alluvial aquifer in the foothill Alpine zone, in Piedmont. They differ in terms of hydrodynamic conditions, and in particular, the groundwater flow occurs in fractured rocks, karst rocks and porous sediments, respectively.

The Mt. Amiata aquifer is unconfined, as a whole, and it is hosted in volcanic rocks (Figure 7) characterized by values of hydraulic conductivity *K* in the range 5.0E-06 ÷ 4.6E-05 m/s (Doveri and Menichini, 2017 and references therein).

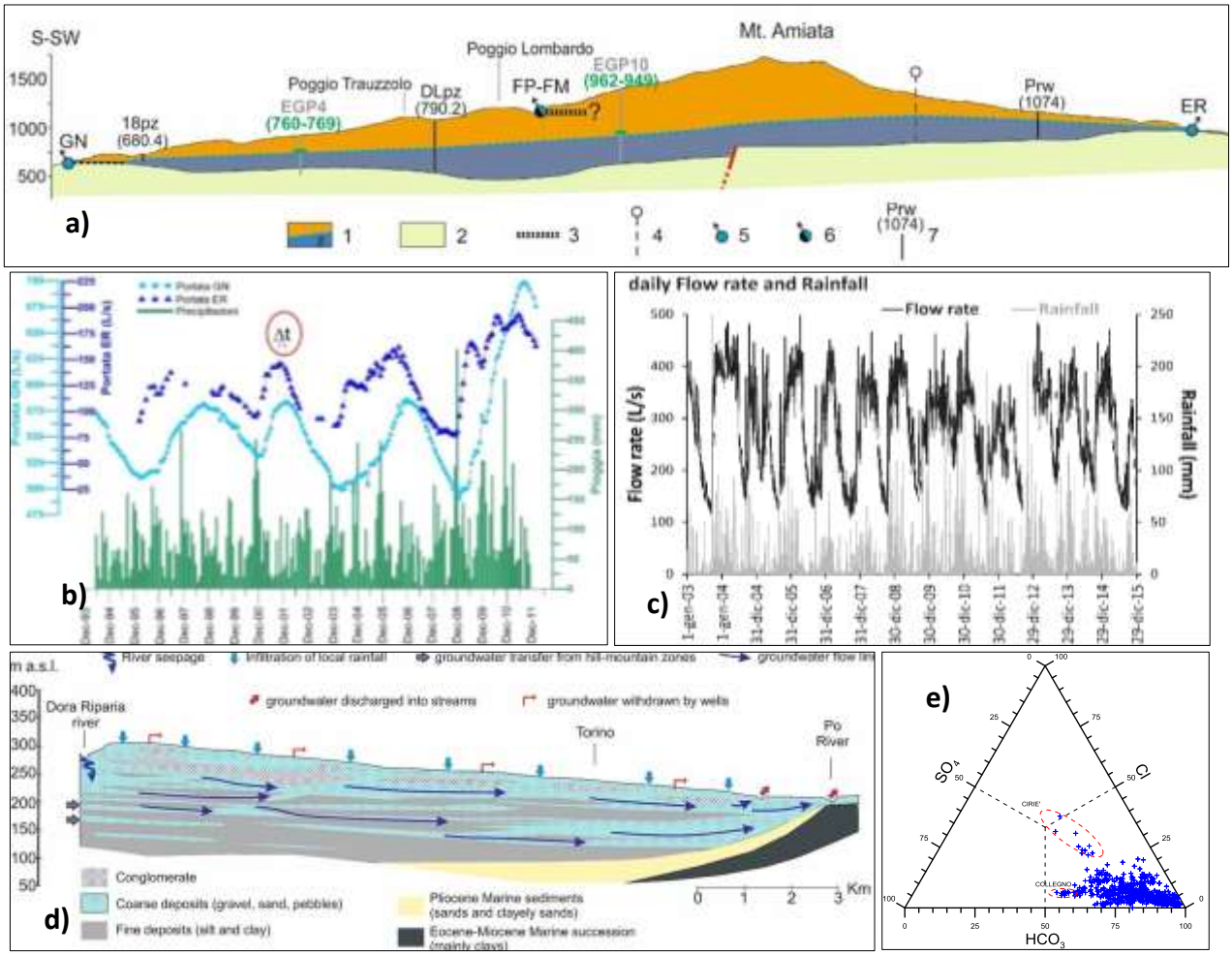

Figure 7. a) *hydrogeological section of the Mt. Amiata aquifer system (Doveri and Menichini, 2017; 1: volcanics – s indicate saturated zone; 2: impervious substratum; 3: local aquitard; 4: groundwater divide; 5: main spring; 6: minor spring; 7: piezometer);* ***b)*** *and* ***c)*** *spring flow rate compared to rainfall for Mt. Amiata and Apuan Alps aquifer systems, respectively (Doveri and Menichini, 2017; Doveri et al., 2018a);* ***d)*** *and* ***e)*** *respectively, schematic model of groundwater input/output and triangular plots of anions abundance, both referred to the foothill aquifer system of the Piedmont Alps area.*

The recharge is of the order of 50-55E06 m^3/y and, in first instance, such value is consistent with the total output at springs. Most springs are at the contact between volcanic rocks and the shaly substratum of the volcanic edifice. Major springs are characterized by flow rate of hundreds L/s. The

unsaturated thickness and the hydrodynamic conditions in the aquifer system produce water-infiltration effects on groundwater through pluriannual cycles of increase-decrease of piezometric levels and flow rates at major springs. The wide range of isotopic values showed by the ensemble of springs point out different average altitude and exposure (seaward, from where most meteoric perturbation arrives, or inland ward) of several recharge areas that feed the respective springs. Groundwater are chiefly of the Ca-Na-K-HCO_3 type and very low salinity, thus indicating that the chemistry is essentially affected by water interaction with the volcanic rocks (Lelli, 2017, and references therein).

The Apuan Alps contain several explicative cases of metamorphic carbonate aquifers (Doveri et al, 2018*b* and references therein). The high rainfall rate (up to 3000 mm/y in the ridge zones), and the permeability of the outcropping carbonate rocks (i.e. marble, dolomitic marble and dolomite) result in a figurative "groundwater tower" (5.6 m^3/s in average as total discharge through the karst springs). Groundwater are mainly of the Ca-HCO_3 type and low salinity. With the exception of local situations, the Apuan metamorphic aquifers are characterized by a deep karst hydrodynamic behaviour, as shown by springs that have a high variability of both flow rates and geochemical characteristics (Figure 7). The monitoring of springs clearly suggests a weak storage capacity for supplying the base flow, thus leading to early breakthrough of low flow at springs following the wet season (November-April). The general variability of water isotopes signatures, observed over time at springs, is in agreement with this conceptual model, considering it requires relatively short transit times of the groundwater flow drained by the springs. Overall, these features make the aquifers highly vulnerable to contamination, and particularly sensitive to climate changes.

The aquifer system that develops in the foothill Alpine zone, beneath the Torino Plain, is considered the most important reservoir in the Torino Province (Bove et al., 2005). It consists of a multilayer that has a phreatic aquifer overlying a succession of impermeable and permeable layers, in which groundwater flow generally occurs in confined to semi-confined conditions. The aquifer layers mainly develop in gravel, sandy gravel and pebbles of fluvial and fluvio-glacial origin. The hydraulic conductivity ranges from 5E-04 to 5E-03 m/s for the phreatic aquifer, and from 4E-05 to 4E-04 m/s for the confined aquifers (De Luca and Osella, 2014). The aquifer system is fed by diffuse infiltration of rainfall, river seepage and transfers of groundwater that originate in upland zones (Figure 7). The outputs of groundwater are for exploitation by wells and for drainage operated by rivers, in the lower part of the plain. Groundwater are mainly of the Ca(Mg)-HCO_3 type with a relatively low salinity for both unconfined and confined aquifers, although the phreatic aquifer hosts groundwater with a relatively higher salinity.

Trend of groundwater quantity and quality and chemical background

The trends analysis on monitoring data was performed on significant points and parameters. The results highlighted some trends over decades. One of the most significant is the decreasing of groundwater yield registered in central Apennines for the volcanic aquifer of Mt. Amiata over the 1990-2010 period (Figure 8), which has been followed by a recovery of flow rates in the successive six-seven years. A qualitative relationship between this behaviour with the evolution of effective rainfall has been preliminary individuated. Although less noteworthy, another trend on

groundwater quantity is the increasing of piezometric levels registered over the last decade in the foothill Alpine zone. In this case, the absence of a significant trend for the effective rainfall, suggests the groundwater trend is mainly tied to a decreasing of groundwater exploitation.

From a water quality point of view, local geochemical background thresholds were defined for significant compounds. Some trends of the physical-chemical and chemical features were also individuated. The most significant are the increase in the Cl concentration observed in some monitored springs of the Mt. Amiata aquifer and the decrease of Cl and NO_3 concentrations observed in the upstream zone of the foothill aquifer in the Alpine zone (Figure 9).

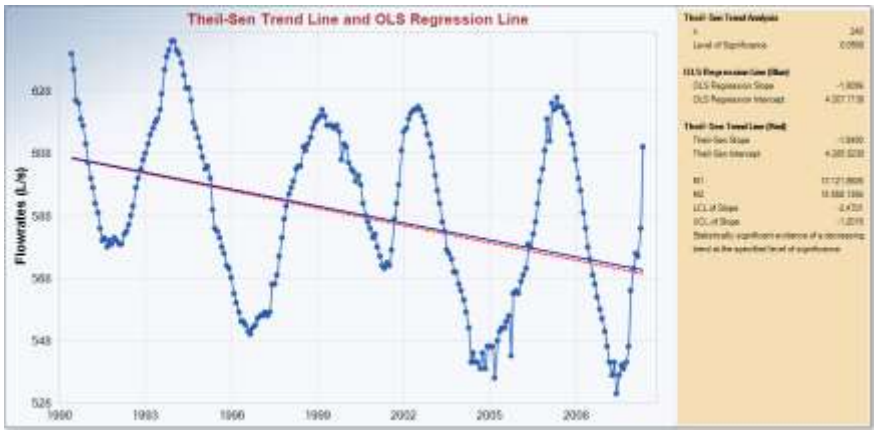

Figure 8. *Time series and trends of flowrates concerning the main Mt. Amiata spring.*

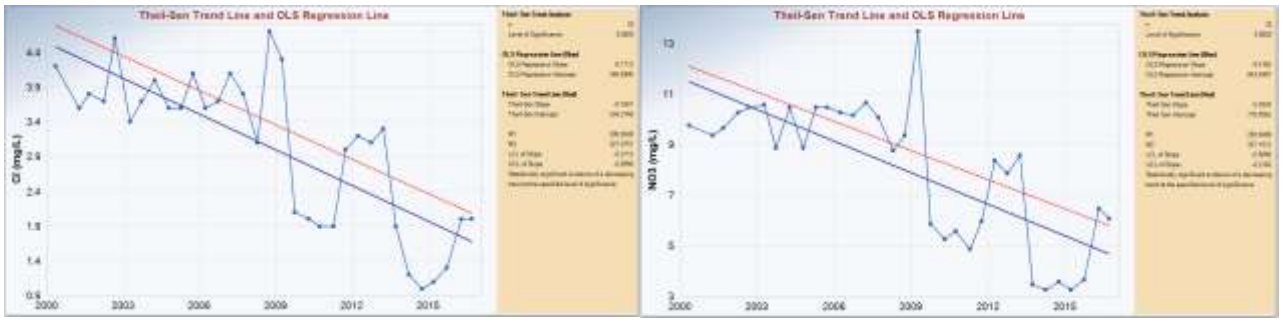

Figure 9. *Time series and trends of chemical compounds concentrations in groundwater flowing in the upper zone of the Torino Plain.*

Numerical models of groundwater quantity and flow

A finite-difference numerical groundwater flow model was done for the Alpine foothill aquifer, both in steady-state (average flow conditions over the last 15 years) and transient conditions (variable flow conditions over the period 2011-2015). The system was discretized with 100 rows, 100 columns and 3 layers, which represent the shallow phreatic aquifer, the underlying aquitard, and the lower semi-confined aquifer system (Figure 10). The Po river level was implemented using a Constant Head boundary condition, whereas at the western borders, where the conceptual model indicates a groundwater inflow component, a General Head Boundary (GHB) was applied. For these boundaries, data from monitoring stations (www.arpa.piemonte.it) and piezometric maps (Bove et al., 2005) were used. The others boundaries, at North and South, were set as no-flow. The diffuse recharge was applied at layer 1 as effective infiltration rate, taking into account the land use (average value of 300 mm/year for urban area and 450 mm/year for rural ones). Main rivers flowing

across the model domain were implemented by the river package based on data of the respective hydrometric stations. More than 100 wells for drinking water and more than 600 wells for other uses were involved in the model, with pumping rates defined according to the indications of the Water Authority, and in some cases, estimating the values from typical range of withdrawals. For calibrating the steady-state model, the mean values of water head recorded by 8 automatic stations located in the area were used (Figure 10).

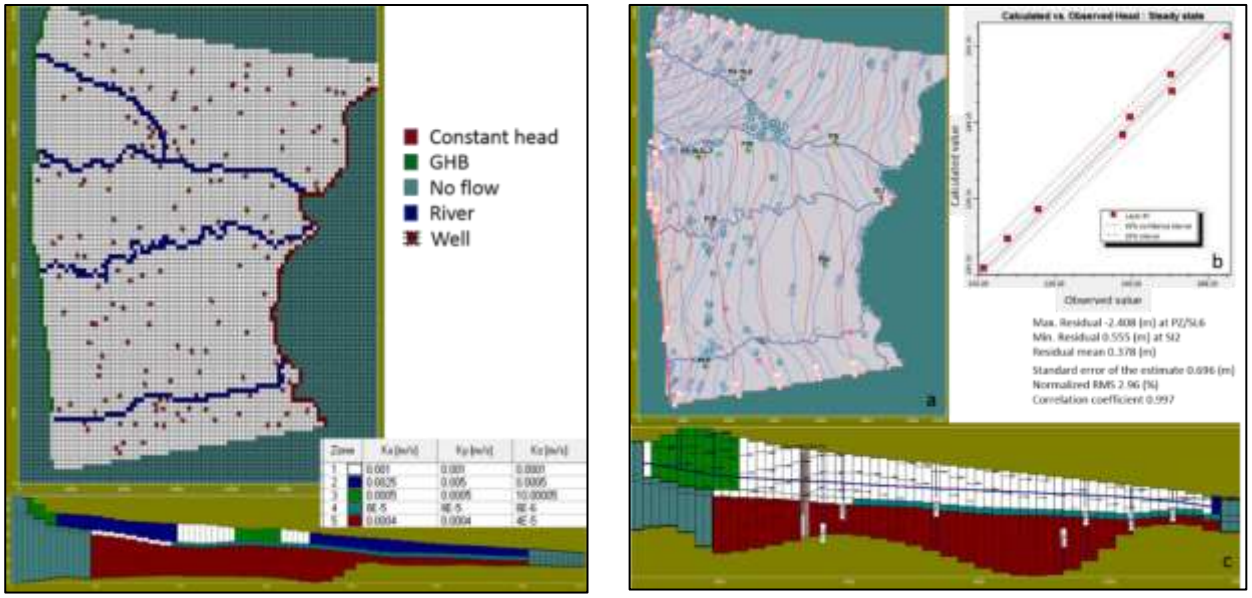

Figure 10. *Left - spatial discretization of the aquifer, boundary conditions and hydraulic conductivity zones in the numerical model. Right - results from the steady-state model: a) Experimental (blue contour) and modeled (red contour) piezometric map (green symbols represent the calibration points); b) Calculated vs Observed piezometric levels at calibration points; c) Flow velocity vectors in the row 66 of the model.*

Results from the steady-state model was the base for developing the transient-state model referred to the 2011-2015 period. Boundary conditions, sinks and sources were monthly discretized using the data of monitoring stations. The transient model allowed reproducing the variability of piezometric levels over time (Figure 11).

As regards the Mt. Amiata and Apuan Alps aquifers, some regression models were developed for main springs, thus reproducing the evolution of their flow rates (Figure 11).

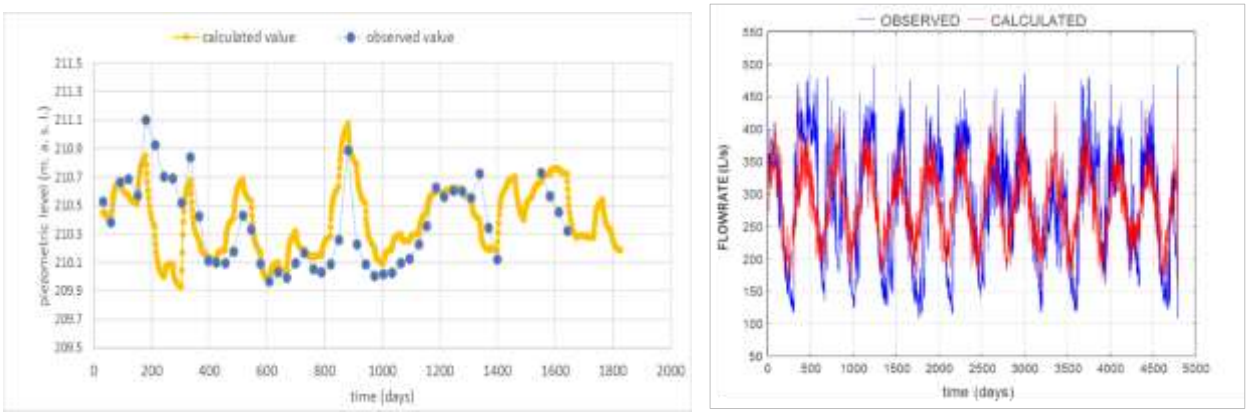

Figure 11. *Left - Observed and calculated piezometric level for a monitoring well of the Alpine foothill aquifer system (from physically-based modelling; transient-state). Right – Observed and calculated flow rate for a main spring of the Apuan Alps aquifer system (from statistical modelling).*

7.3.4 Conclusions

Within the NextData project, a significant contribution in terms of groundwater knowledge was provided. Data collection, elaboration and modelling regarded three of the main aquifer systems extending in Italian mountain zones. Thanks to these activities, a large number of data was properly filtered and made available by means of the NextData web-platform. Specific results and information concerning the examined systems were also delivered by pointing out processes, mechanisms and trends affecting groundwater quality and quantity, as well as by developing numerical models able to reproduce the evolution of groundwater flow and yield. Furthermore, approaches of work as reference strategies for investigating aquifers were presented.

7.4 Remote sensing applications for monitoring of paraglacial processes

P. Allasia[1], F. Ardizzone[1], D. Giordan2, M. Cignetti[2], M. Manunta[2]

[1]CNR-IRPI, National Research Council of Italy, Research Institute for Geo-Hydrological Protection, Perugia, Italy
[2]CNR-IRPI, National Research Council of Italy, Research Institute for Geo-Hydrological Protection, Torino, Italy
[3]CNR-IREA, National Research Council of Italy, Institute for the Electromagnetic Detection of the Environment, Napoli, Italy

7.4.1 Introduction

Periglacial, paraglacial and proglacial processes and systems play an important role in high mountain landscapes evolution (Knight and Harrison 2009; Carrivick and Heckmann 2017).

In alpine regions, the definition of ground surface displacements is a key issue for the identification of active geomorphological processes, and their evolution. In the last decades, several consolidated monitoring techniques were exploited for periglacial (Kääb et al., 2003) and glacial processes (Giordan et al., 2016). The advanced remote sensing techniques, as Differential Synthetic Aperture Radar Interferometry (DInSAR) (Ferretti et al., 2001; Berardino et al., 2002; Hooper et al., 2004), have upgraded the information available on ground deformation generating ground velocity maps and long time series of ground deformation. The current increase in multi-temporal acquisition availability (e.g. ERS-1/2, ENVISAT, RADARSAT-1, Sentinel-1) ensures an extensive spatial and temporal coverage, able to furnish information in different physiographic and geographic areas, also for those areas with limited or difficult assess. However, some intrinsic limitation are to be considered: *i)* coherence loss due to large revisit time; *ii)* phase decorrelation due to large or rapid displacement; *iii)* line-of-site (LOS) measurements only; *iv)* atmospheric phase screen (APS), amplified in high mountain gradient; *v)* temporal coherence loss due to snow cover. Furthermore, high mountain landscape entails some additionally challenges i.e. high topographic gradients associated with the complex orography, abundant vegetation affecting temporal correlation of the SAR signal, and unsuitable valley flanks orientations relative to the SAR view angle (Colesanti and Wasowski, 2006; Cigna et al., 2013). Some recent tools i.e. ESA Grid-based operational environment support the SAR data processing by the unsupervised implementation of the Parallel-SBAS (P-SBAS) algorithm (Casu et al. 2014). This web-interface tool performs the full SBAS-DInSAR processing chain

in an unsupervised fashion from the raw SAR images to the generation of ground velocity maps and the related time series (De Luca et al., 2015).
A combination of diverse SAR images acquisition (e.g. ERS-1/2, ENVISAT-ASAR, Sentinel-1) and an effective comparison of data also obtained by different DInSAR technique, was applied to the Aosta Valley region (northwestern Italy), a study area characterized by the presence of many active geomorphological processes (e.g. glaciers, rock glaciers).

7.4.2 The Italian Western Alps

The Aosta Valley region (AVr) is located in the northwestern of Italy (Figure 12). Elevation ranges from about 400 m a.s.l. to over 4800 m a.s.l.

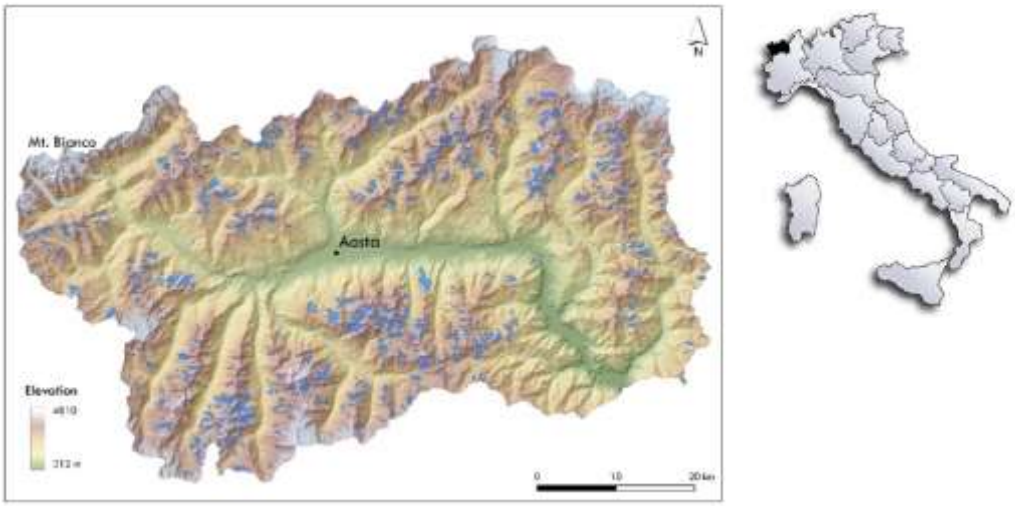

Figure 12. *Relief terrain of the Aosta Valley region (northwestern Italy); light blue polygons correspond to the present glaciers, and the blue polygon represent the rock glaciers location.*

The Aosta Valley glaciers represent one-third of the Italian glaciers (Diolaiuti et al., 2012), and cover about 5% of the regional territory (Catasto Ghiacciai - http://catastoghiacciai.regione.vda.it/Ghiacciai/MainGhiacciai.html). Generally, the alpine permafrost shows a fragmented distribution, with a typical creep deformation related to the permafrost temperature (Delaloye et al., 2010). Rock glaciers (RGs), which occupy about 2% of the regional territory (Guglielmin and Smiraglia, 1997) represent a common periglacial landform of the Aosta Valley region.

7.4.3 DInSAR techniques application

Mean velocity maps and ground deformation time series have been generated taking advantage of the G-POD service (Cignetti et al., 2016) based on SAR images processing. The Envisat AVASAR available data have been processed by the P-SBAS technique (Casu et al. 2014), both in ascending and descending orbits. The period of observation ranges from June 2004 and October 2010 for the ascending orbit, and from September 2004 and October 2010 for the descending orbit.
The available tracks cover the main part of the regional territory, excluding only the eastern part of the region (about 10%) (Figure 13).

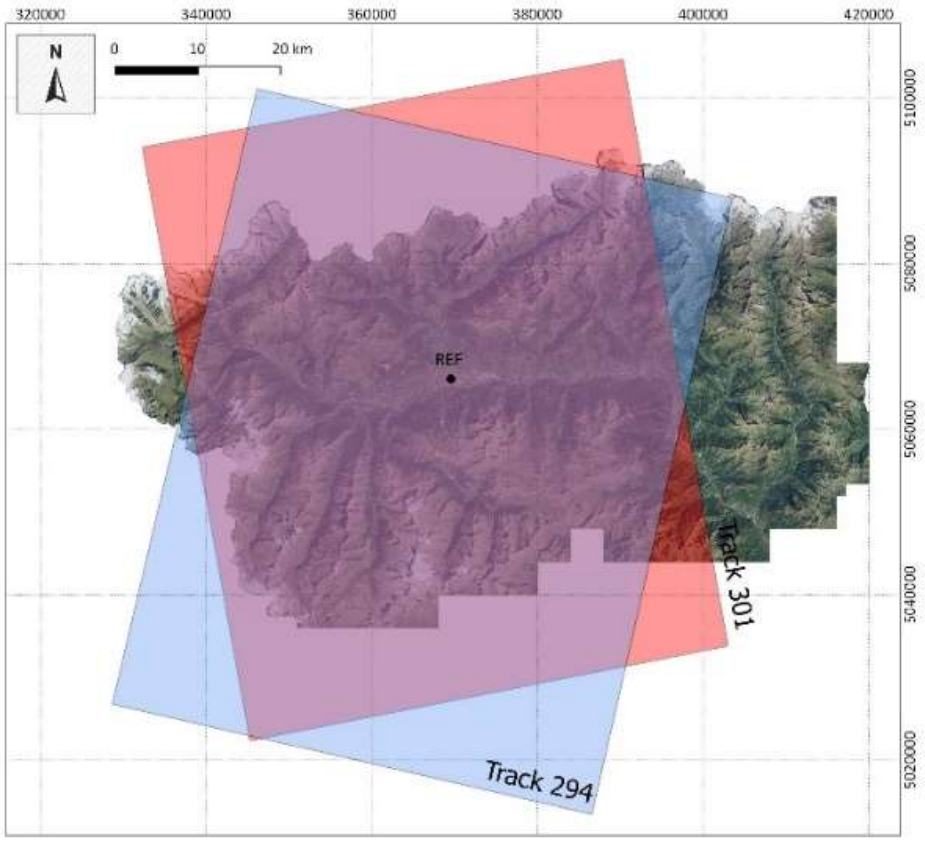

Figure 13. *Map of the AVr (in light grey) respect to the ENVISAT ASAR track extent for both ascending (Track n°301) and descending (Track n° 294) orbit. The black dot represents the reference point location.*

To obtain reliable and favorable results, we performed an informed choice of SAR images, based on the comparison with the available meteorological data (i.e. height of snow, rainfall picks). By this way, we tried to minimize the temporal decorrelation effects mainly related to the snow cover, preserving the largest number of SAR acquisitions.

7.4.4 AVr results

The achieved results are collected and organized in a Geographic Informatics System (QGIS Development Team 2009) environment. The coherent targets (33086 for ascending orbit, 20317 for descending orbit) cover the main part of the regional territory, covering a time interval of about 6 years (Figure 14). The highest portion of the lateral valley was excluded to the coverage because these sectors corresponding to the glaciated areas, affected by decorrelation effect due to the large displacement of glaciers.

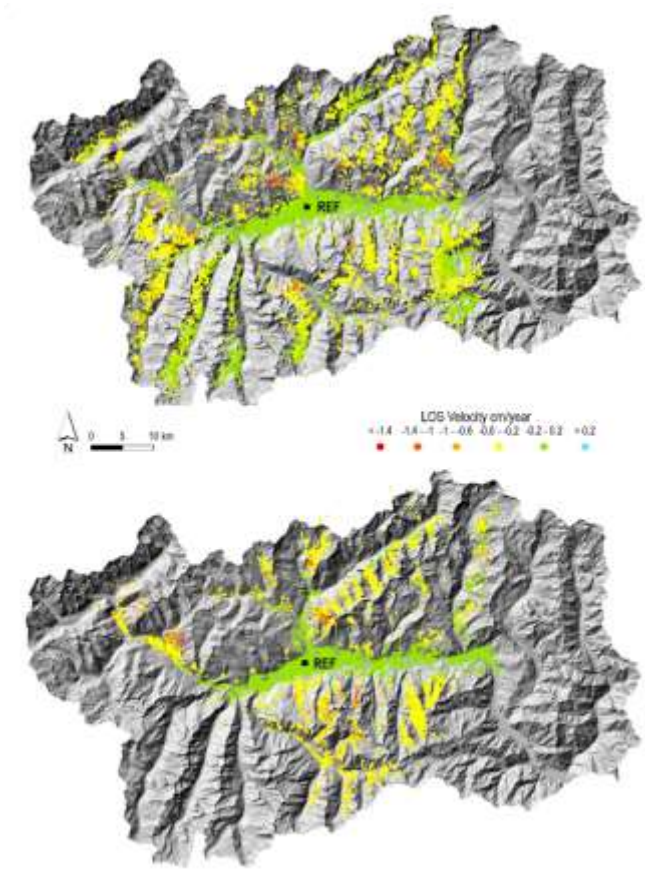

Figure 14. *Mean velocity maps measured along the satellite LOS for the Envisat dataset: a) Ascending orbit data, b) Descending orbit data*.

The number of RGs covered by the SBAS targets are 123 (on 937 in total) for ascending orbit, and 65 for descending orbit. In the case of RGs, we analyzed all the active, inactive and relict forms. Generally, the mean velocity maps analysis highlights good agreement with the state of activities of the inventoried RGs. Specifically, the time series provide the analyze eventual RGs activation and/or seasonal deformations over the observed period (Figure 15).

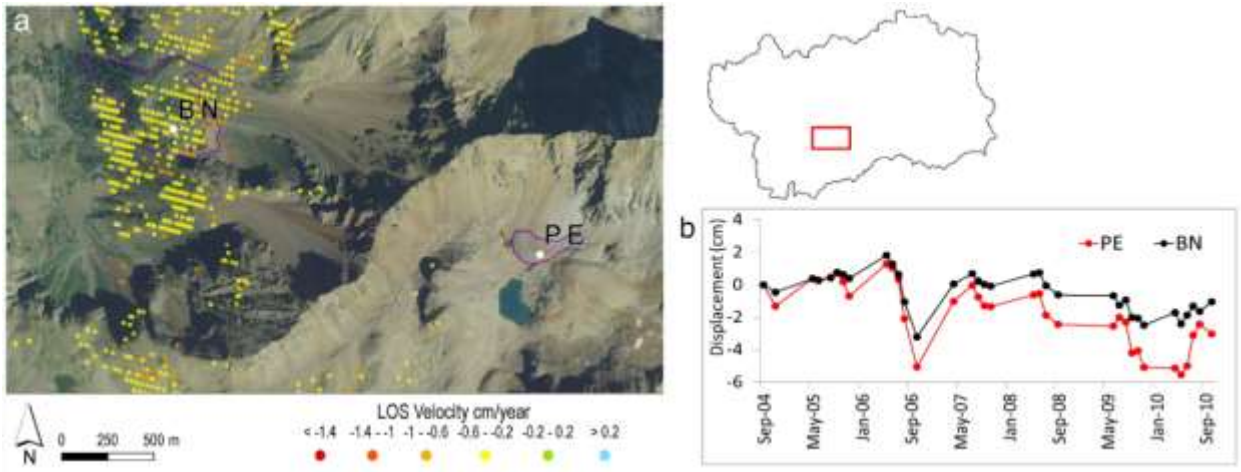

Figure 15. *Rock glaciers deformation measurement: a) surface velocities measured for the Becca di Nona (BN), and Petite Emilius (PE) rgs, in descending orbit; b) time series corresponding to the targets signed by white dots in the above map. The time series dysplay a general constant deformmation range, with a sort of acceleration during the summer to early autumn months, with maximum displacement of -1.4 cm from September 2004 to October 2010.*

7.4.5 Data validation

In order to validate the obtained results, we compare the SBAS targets with the Permanent Scatterers available on the "*Portale Cartografico Nazionale*". The PSs have been processed by the TRE Europa by the PSInSAR techniques as part of a National Project (http://www.pcn.minambiente.it/mattm/progetto-piano-straordinario-di-telerilevamento/). The data are not downloadable, so we manually extract the time series values reported in table format within the portal. Firstly, we analysed a stable area with high coherent targets (Figure 16). Then we compared a numer of targets presenting ground deformation in correspondance of a RG (Figura 17). A good agreement between the selected SBAS targets and PSs surface deformation rates have been observed, and a comparable distribution con be observed.

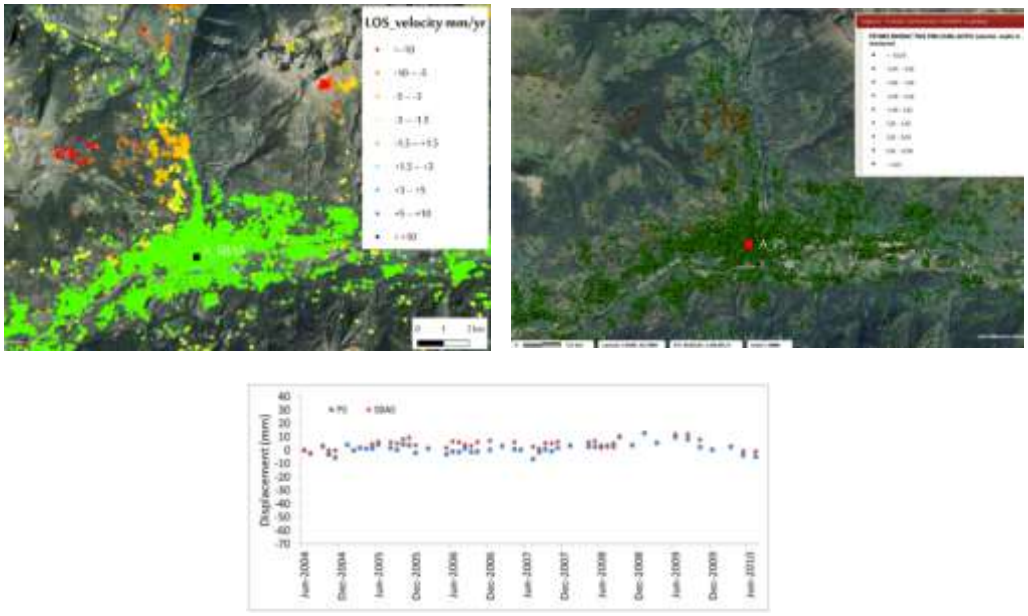

Figure 16. *GPOD results validation: a) comparison between the ENVISAT ascending SBAS resutls, and the PSInSAR results over the Aosta municipality.*

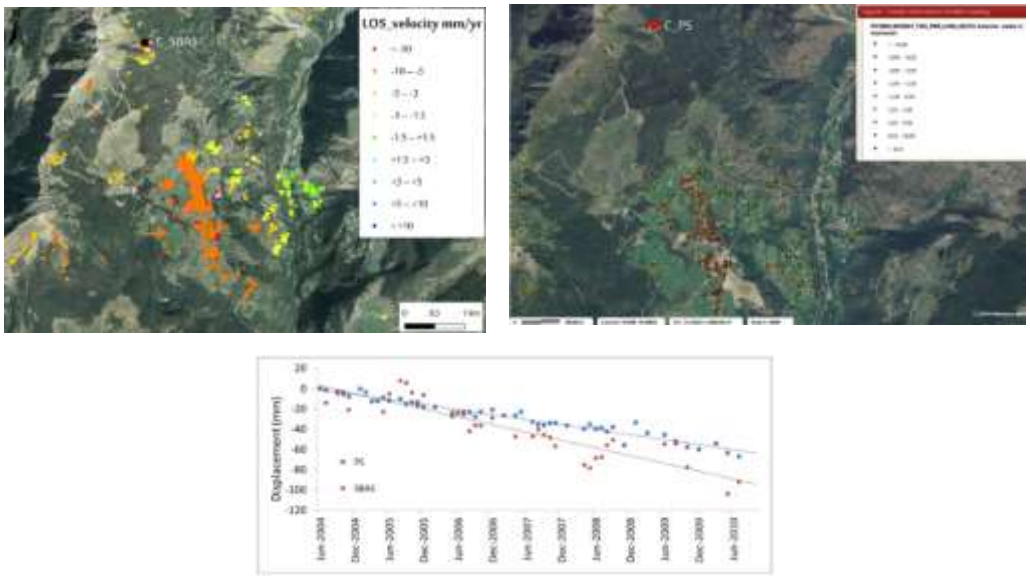

Figure 17. *GPOD results validation: a) comparison between the ENVISAT ascending SBAS resutls, and the PSInSAR results over the Mont Meabèrg (Valtourenenche valley).*

7.4.6 Conclusions

DInSAR technique allows to generate long-term surface deformation time series and surface velocities maps. The technique is very useful also for hardly accessible areas as high-mountain regions. Deformation time series are an important tool for the identification and characterization of active gravitational processes. The use of these data is well-known for landslides monitoring, but is also adopted for glaciers, paraglacial, and periglacial processes. In this work, we present in particular the use of DInSAR processing for active rock glaciers monitoring. We focus our attention on the use of free SAR images processing. We developed a methodology taking advantage of the ESA G-POD service (Cignetti et al., 2016). This approach is an important application of available ENVISAT ASAR dataset, and can be implemented with Sentinel-1 costellation. The high-revisit time of Sentinel-1 cab be useful also for the carachterization of kinematic behavior of paralgacial and periglacial processes that tipically present a seasonall trend.

References

Amponsah W., Marchi L., Zoccatelli D., Boni G., Cavalli M., Comiti F., Crema S., Lucía A., Marra F., Borga M., 2016. Hydrometeorological characterisation of a flash flood associated with major geomorphic effects: Assessment of peak discharge uncertainties and analysis of the runoff response. J. of Hydrom., 17:3063-3077.

Auer I., Bohm R., Jurkovic A., Lipa W., Orlik A., Potzmann R., Schöner W., Ungersböck M., Matulla C., Briffa K., Jones P., Efthymiadis D., Brunetti M., Nanni T., Maugeri M., Mercalli L., Mestre O., Moisselin J. –M., Begert M., Müller-Westermeier G., Kveton V., Bochnicek O., Stastny P., Lapin M., Szalai S., Szentimrey T., Cegnar T., Dolinar M., Gajic-Capka M., Zaninovic K., Majstorovic Z., Nieplova E., 2007. HISTALP—historical instrumental climatological surface time series of the greater Alpine region 1760–2003. Int. J. Climatol., 27:17–46.

Barnett T. P., Adam J. C., Lettenmaier D. P., 2005. Potential impacts of a warming climate on water availability in snow-dominated regions. Nature, 438:303–309.

Bartolini E., Claps P., D'Odorico P., 2001. Connecting European snow cover variability with large scale atmospheric patterns. Adv. Geosci., 26:93–97.

Beniston M., 1997. Variations of snow depth and duration in the Swiss Alps over the last 50 years: links to changes in large-scale climatic forcings. Clim. Change, 36:281–300.

Beniston M., 2012. Is snow in the Alps receding or disappearing? Wiley Interdiscip. Rev. Clim. Change, 3:349–358.

Berardino P., Fornaro G., Lanari R., Sansosti E., 2002. A new algorithm for surface deformation monitoring based on small baseline differential SAR interferograms. IEEE Trans Geosci Remote Sens 40:2375–2383. Doi: 10.1109/TGRS.2002.803792.

Birsan M.V., Molnar P., Burlando P., Pfaundler M., 2005. Streamflow trends in Switzerland. J Hydrol., 314:312–29.

Bove A., Casaccio D., Destefanis E., De Luca D. A., Lasagna M., Masciocco L., Ossella L., Tonussi M., 2005. Idrogeologia della pianura piemontese. Regione Piemonte Direzione Pianificazione delle Risorse Idriche, Mariogros Industrie Grafiche S.p.A., Torino.

Brocca L., Melone F., Moramarco T., 2011. Distributed rainfall-runoff modelling for flood frequency estimation and flood forecasting, Hydrol. Proc., 25:2801–2813.

Brunetti M., Lentini G., Maugeri M., Nanni T., Auer I., Böhm R., Schöner W., 2009. Climate variability and change in the Greater Alpine Region over the last two centuries based on multi-variable analysis. Int. J. Climatol., 29:2197–225.

Carrivick J. L., Heckmann T., 2017. Short-term geomorphological evolution of proglacial systems. Geomorphology, 287:3–28. Doi: 10.1016/j.geomorph.2017.01.037.

Casu F., Elefante S., Imperatore P., Zinno I., Manunta M., De Luca C., Lanari R., 2014. SBAS-dinsar Parallel Processing for Deformation Time-Series Computation. IEEE J. Sel. Top. Appl. Earth Obs. Remote Sens. Early Access Online: doi: 10.1109/JSTARS.2014.2322671.

Cigna F., Bianchini S., Casagli N., 2013. How to assess landslide activity and intensity with Persistent Scatterer Interferometry (PSI): the PSI-based matrix approach. Landslides 10:267–283. Doi: 10.1007/s10346-012-0335-7.

Cignetti M., Manconi A., Manunta M., Giordan D., De Luca C., Allasia P., Ardizzone F., 2016. Taking Advantage of the ESA G-POD Service to Study Ground Deformation Processes in High Mountain Areas: A Valle d'Aosta Case Study, Northern Italy. Remote Sens., 8:852. Doi: 10.3390/rs8100852.

Colesanti C., Wasowski J., 2006. Investigating landslides with space-borne Synthetic Aperture Radar (SAR) interferometry. Eng. Geol., 88:173–199. Doi: 10.1016/j.enggeo.2006.09.013.

Compo G. P., Whitaker J. S., Sardeshmukh P. D., Matsui N., Allan R. J., Yin X., Gleason B. E., Vose R. S., Rutledge G., Bessemoulin P., Brönnimann S., Brunet M., Crouthamel R. I., Grant A. N., Groisman P. Y., Jones P. D., Kruk M., Kruger A. C., Marshall G. J., Maugeri M., Mok H. Y., Nordli Ø., Ross T. F., Trigo R. M., Wang X. L., Woodruff S. D., Worley S. J., 2011. The twentieth century reanalysis project. Quarterly J. Roy. Meteorol. Soc., 137:1–28.

Compo G.P., and co–authors, 2015. NOAA/CIRES Twentieth Century Global Reanalysis Version 2c. Research Data Archive at the National Center for Atmospheric Research, Computational and Information Systems Laboratory. http://dx.doi.org/10.5065/D6N877TW (updated yearly).

De Luca D. A., Destefanis E., Forno M. G., Lasagna M., Masciocco L., 2014. The genesis and the hydrogeological features of the Turin Po Plain fontanili, typical lowland springs in Northern Italy. Bull Eng Geol Environ 73:409–427.

De Luca C., Cuccu R., Elefante S., Zinno I., Manunta M., Casola V., Rivolta G., Lanari R., Casu F., 2015. An On-Demand Web Tool for the Unsupervised Retrieval of Earth's Surface Deformation from SAR Data: The P-SBAS Service within the ESA G-POD Environment. Remote Sens., 7:15630–15650. Doi: 10.3390/rs71115630.

Delaloye R., Lambiel C., Gärtner-Roer I., 2010. Overview of rock glacier kinematics research in the Swiss Alps. Geogr. Helvetica, 65:135–145.

Diolaiuti G. A., Bocchiola D., Vagliasindi M., D'Agata C., Smiraglia C., 2012. The 1975-2005 glacier changes in Aosta Valley (Italy) and the relations with climate evolution. Prog. Phys. Geogr. 36:764–785. Doi: 10.1177/0309133312456413.

Dobler C., Burger G., Stotter J., 2012. Assessment of climate change impacts on flood hazard potential in the Alpine Lech watershed. J. Hydrol., 460:29–39.

Doveri M., Menichini M., 2017. Aspetti idrogeologici delle vulcaniti nel Monte Amiata. In: Il Vulcano di Monte Amiata. a cura di Claudia Principe, Guido Lavorini e Luigina M. Vezzoli (eds.), pp. 255 - 265. ESA - Edizioni Scientifiche ed Artistiche, 2017 - Napoli, Italia.

Doveri M., Menichini M., Scozzari A., 2016. Protection of groundwater resources: worldwide regulations, scientific approaches and case study. In: Scozzari A, Dotsika E (edited by): “Threats to the quality of groundwater resources: prevention and control" - The handbook of environmental chemistry, Springer-Verlag Berlin Heidelberg 2016, 40:13-30.

Doveri M., Menichini M., Provenzale A., Scozzari A., 2018a. Groundwater response to climate changes: examples of observed and modeled trends on Tuscany aquifers (central Italy). Rend. Online Acc. Lincei 2018 (in press).

Doveri M., Piccini L., Menichini M., 2018b. Hydrodynamic and geochemical features of metamorphic carbonate aquifers and implications for water management: the Apuan Alps (NW Tuscany-Italy) case study. In: Karst Water Environment: Advances in Research, Management and Policy (T. Younos, M. Schreiber, K. K. Ficco, Editors), vol. 68. Springer International Publishing AG, part of Springer Nature 2019, pp 209-249 (First Online: 27 May 2018)

Durand Y., Giraut G., Laternser M., Etchevers P., Merindol L., Lesaffre N., 2009. Reanalysis of 47 years of climate in the French Alps (1958–2005): climatology and trends for snow cover. J. Appl. Meteorol. Climatol., 48:2487–2512.

Efthymiadis D., Jones P. D., Briffa K. R., Auer I., Böhm R., Schöner W., Frei C., Schmidliand J., 2006. Construction of a 10- min-gridded precipitation data set for the Greater Alpine Region for 1800–2003. J. Geophys. Res. 2006, 110, D01105.

Ferretti A., Prati C., Rocca F., 2001. Permanent scatterers in SAR interferometry. IEEE Trans. Geosci. Remote Sens. 39:8–20.

Francou B., Vuille M., Wagnon P., Mendoza J., Sicart J.–E., 2003. Tropical climate change recorded by a glacier in the central Andes during the last decades of the twentieth century: Chacaltaya, Bolivia, 16°S. J. Geophys. Res., 108, 4154.

Gaume E., Borga M., 2008. Post-flood field investigations in upland catchments after major flash floods: proposal of a methodology and illustrations, J. Flood Risk Management, 1:175–189.

Giordan D., Allasia P., Dematteis N., Dell’Anese F., Vagliasindi M., Motta E., 2016. A Low-Cost Optical Remote Sensing Application for Glacier Deformation Monitoring in an Alpine Environment. Sensors 16:1750. Doi: 10.3390/s16101750.

Guglielmin M., Smiraglia C., 1997. The rock glacier inventory of the Italian Alps. Arch. Com. Glaciol. Ital. 3.

Harbaugh A. W., Banta E. R., Hill M. C., Mcdonald M. G., 2000. MODFLOW-2000, the U.S. Geological Survey modular ground-water model—User guide to modularization concepts and the Ground-water flow process. U.S. Geological Survey Open-File Report 00-92, 121 p.

Hooper A., Zebker H., Segall P., Kampes B., 2004. A new method for measuring deformation on volcanoes and other natural terrains using insar persistent scatterers: A NEW PERSISTENT SCATTERERS METHOD. Geophys. Res. Lett. 31:. Doi: 10.1029/2004GL021737.

Hurrell J., 1995. Decadal trends in the North Atlantic Oscillation regional temperatures and precipitation. Science, 269:676–679.

Huss M., Hock R., Bauder A., Funk M., 2010. 100-year mass changes in the Swiss Alps linked to the Atlantic Multidecadal Oscillation. Geophys. Res. Lett., 37, L10501.

IPCC, 2013. Summary for policymakers. In: Climate Change 2013: The Physical Science Basis. Contribution of Working Group I to the Fifth Assessment Report of the Intergovernmental Panel on Climate Change [Stocker, T.F., D. Qin, G.-K. Plattner,M. Tignor, S. K. Allen, J. Boschung, A. Nauels, Y. Xia, V. Bex and P.M. Midgley (eds.)]. Cambridge University Press, Cambridge, United Kingdom and New York, NY, USA.

Kääb A., Kaufmann V., Ladstädter R., Eiken T., 2003. Rock glacier dynamics: implications from high-resolution measurements of surface velocity fields. In: Eighth International Conference on Permafrost. Balkema, pp 501–506.

Kaser G., Hardy D. R., Mölg T., Bradley R. S., Hyera T. M., 2004. Modern glacier retreat on Kilimanjaro as evidence of climate change: Observations and facts. Int. J. Climatol., 24-329–339.

Kaser G., Großhauser M., Marzeion B., 2010. Contribution potential of glaciers to water availability in different climate regimes. Proc Natl Acad Sci USA, 107:20223–20227.

Knight J., Harrison S., 2009. Periglacial and paraglacial processes and environments. Geological Society of London.

Laternser M., Schneebeli M., 2003. Long-term snow climate trends of the Swiss Alps (1931–99). Int. J. Climatol., 23:733–750.

Lelli M., 2017. Caratterizzazione chimica delle acque circolanti all'interno del Complesso Vulcanico del Monte Amiata. In "Il vulcano di Monte Amiata", Eds. C. Principe, G. Lavorini, L. Vezzoli, pp. 267-280.

Lionello P. (Ed.), 2012. The Climate of the Mediterranean Region, From the Past to the Future. Elsevier, Amsterdam, Netherlands, 502 pp.

Marchi L., Borga M., Preciso E., Sangati M., Gaume E., Bain V., Delrieu G., Bonnifait L., Pogačnik N., 2009. Comprehensive post-event survey of a flash flood in Western Slovenia: observation strategy and lessons learned. Hydrol. Proc., 23:3761-3770.

Marty C., 2008. Regime shift of snow days in Switzerland. Geophys. Res. Lett., 35, L12501.

Mayer T. D., Naman S. W., 2011. Streamflow response to climate as influenced by geology and elevation. J. Am. Water Resour. Assoc., 47:724–38.

Mitchell T. D., Jones P. D., 2005. An improved method of constructing a database of monthly climate observations and associated high-resolution grids. Int. J. Climatol., 25:693–712.

Moore J. N., Harper J. T., Greenwood M. C., 2007. Significance of trends toward earlier snowmelt runoff, Columbia and Missouri Basin headwaters, western United States. Geophys. Res. Lett., 34, L16402.

Nash J.E., Sutcliffe J.V., 1970. River flow forecasting through conceptual models, Part I: A discussion of principles. J. Hydrol., 10(3):282-290.

Pederson G. T., Gray S. T., Ault T., Marsh W., Fagre D. B., Bunn A. G., Woodhouse C. A., Graumlich L. J., 2011. Climatic controls on the snowmelt hydrology of the Northern Rocky Mountains. J. Climate, 24:1666–1687.

Perkins S.E., Alexander L.V., Nairn J.R., 2012. Increasing frequency, intensity and duration of observed global heatwaves and warm spells. Geophys. Res. Lett. 39, L20714.

Pfister C., Weingartner R., Luterbacher J., 2006. Hydrological winter droughts over the last 450 years in the Upper Rhine basin: a methodological approach. Hydrol. Sci. J., 51:966–985.

Poli P., Hersbach H., Dee D. P., Berrisford P., Simmons A. J., Vitart F., Laloyaux P., Tan D. G., Peubey C., Thépaut J., Trémolet Y., Hólm E. V., Bonavita M., Isaksen L., Fisher M., 2016. ERA-20C: An Atmospheric Reanalysis of the Twentieth Century. J. Climate, 29:4083-4097, Doi: 10.1175/JCLI-D-15-0556.1.

QGIS Development Team, 2009. QGIS Geographic Information System. Open Source Geospatial Foundation.

Razali N.M., Wah Y.B., 2011. Power comparisons of Shapiro-Wilk, Kolmogorov-Smirnov, Lilliefors and Anderson-Darling tests. Journal of Statistical Modeling and Analytics, 2(1):21-33.

Rosner B., 1975. On the detection of many outliers. Technometrics, 17:221-227.

Rosner B., 1983. Percentage points for a generalized ESD many-outlier procedure. Technometrics, 25:165-172.

Rousseeuw P.J., Leroy A.M., 1987. Robust Regression and Outlier Detection. John Wiley.

Russo S., Dosio A., Graversen R. G., Sillmann J., Carrao H., Dunbar M. B., Singleton A., Montagna P., Barbola P., Vogt J. V., 2014. Magnitude of extreme heat waves in present climate and their projection in a warming world. J. Geophys. Res. Atmos. 119:12500–12512.

Russo S., Sillmann J., Fischer E., 2015. Top ten European heatwaves since 1950 and their occurrence in the coming decades. Environ. Res. Lett., 10, 124003.

Scherrer S. C., Wüthrich C., Croci-Maspoli M., Weingartner R., Appenzeller C., 2013. Snow variability in the Swiss Alps 1864–2009. Int. J. Climatol., doi:10.1002/joc.3653.

Scherrer S. C., Appenzeller C., 2006. Swiss Alpine snow pack variability: major patterns and links to local climate andnlarge-scale flow. Clim. Res., 32:187–199.

Scherrer S. C., Appenzeller C., Laternser M., 2004. Trends in Swiss Alpine snow days: the role of local- and large-scale climate variability. Geophys. Res. Lett., 31, L13215.

Schlesinger M. E., Ramankutty N., 1994. An oscillation in the global climate system of period 65–70 years. Nature, 367:723–726.

Sen P. K. 1968. Estimates of the regression coefficient based on Kendall's tau. Journal of the American Statistical Association, 63:1379–1389.

Seneviratne S.I., Corti T., Davin E. L., Hirschi M., Jaeger E. B., Lehner I., Orlowsky B., Teuling A. J., 2010. Investigating soil moisture-climate interactions in a changing climate: a review. Earth Sci. Rev., 99:125–161.

Serquet G., Marty C., Dulex J.–P., Rebetez M., 2011. Seasonal trends and temperature dependence of the snowfall/precipitation-day ratio in Switzerland. Geophys Res Lett, 38, L046976.

Sinclair A.J., 1986. Statistical interpretation of soil geochemical data, 97-115. In: Exploration geochemistry: design and interpretation of soil surveys. (W.K. Fletcher, S.J. Hoffman, M.B.)

Singh A., Nocerino J.M., 1995. Robust Procedures for the Identification of Multiple Outliers. Handbook of Environmental Chemistry, Statistical Methods, Vol. 2.G, pp. 229-277. Springer Verlag, Germany.

Stahl K., Hisdal H., Hannaford J., Tallaksen L. M., van Lanen H. A. J., Sauquet E. Demuth S., Fendekova M., Jódar J., 2010. Streamflow trends in Europe: evidence from a dataset of near-natural catchments. Hydrol. Earth Syst. Sci., 14:2367–2382.

Sutton R. T., Dong B., 2012. Atlantic Ocean influence on a shift in European climate in the 1990s. Nature Geosci., 5:788–792.

Tague C., Grant G. E., 2009. Groundwater dynamicsmediate low-flow response to global warming in snow-dominated alpine regions. Water Resour Res., 45, W07421.

Taylor R., Scanlon B., Doll P., Rodell M., van Beek R., Wada Y., Longuevergne L., Leblanc M., Famiglietti J. S., Edmunds M., Konikow L., Green T. R., Chen J., Taniguchi M., Bierkens M. F. P., MacDonald A., Fan Y., Maxwell R. M., Yechieli Y., Gurdak J. J., Allen D. M., Shamsudduha M., Hiscock K., Yeh P. J.-F., Holman I., Treidel H., 2013. Ground water and climate change. Nature climate change, 3:322-329.

Trenberth K E, Jones P. D., Ambenje P., Bojariu R., Easterling D., Klein Tank A., Parker D., Rahimzadeh F., Renwick J. A., Rusticucci M., Soden B., Zhai P., 2007. Observations: surface and atmospheric climate change Climate Change 2007: The Physical Science Basis. Contribution of Working Group I to the Fourth Assessment Report of the Intergovernmental Panel on Climate Change ed S Solomon, D Qin, M Manning, Z Chen, M Marquis, K B Averyt, M Tignor and H L Miller (Cambridge: Cambridge University Press).

Valt M., Cianfarra P., 2010. Recent snow cover variability in the Italian Alps Cold Reg. Sci. Technol., 64:146–157.

Vautard R., Yiou P., D'Andrea F., de Noblet N., Viovy N., Cassou C., Polcher J., Ciais P., Kageyama M., Fan Y., 2007. Summertime European heat and drought waves induced by wintertime Mediterranean rainfall deficit. Geophys. Res. Lett., 34, L07711.

Zampieri M., D'Andrea F., Vautard R., Ciais P., de Noblet-Ducoudre N., Yiou P., 2009. Hot European summers and the role of soilmoisture in the propagation of Mediterranean drought. J. Climate, 22:4747–4758.

Zampieri M., Scoccimarro E., Gualdi S., 2013. Atlantic influence on spring snowfall over Alps in the last 150 years. Environ. Res. Lett. 8 (3).

Zampieri M., Scoccimarro E., Gualdi S., Navarra A., 2015. Observed shift towards earlier spring discharge in the main Alpine rivers. Sci. Total Environ., 503:222–232.

Zampieri M., Russo S., di Sabatino S., Michetti M., Scoccimarro E., Gualdi S., 2016. Global assessment of heat wave magnitudes from 1901 to 2010 and implications for the river discharge of the Alps. Sci. Total Environ, 571: 1330–1339.

Wilcox Rand R., 2001. "Theil–Sen estimator", Fundamentals of Modern Statistical Methods: Substantially Improving Power and Accuracy, Springer-Verlag, pp. 207–210, ISBN 978-0-387-95157-7.